CEAI, Vol. 8, No. 1, pp. 33-41, 2006 Printed in Romania

A STUDY ON WORKSPACE TOPOLOGIES OF 3R INDUSTRIAL-TYPE MANIPULATORS

Erika Ottaviano *, Manfred Husty **, Marco Ceccarelli ***

** LARM, University of Cassino Via Di Biasio 43, 03043 Cassino (Fr), Italy email: ottaviano@unicas.it*
** Institute for Engineering Mathematics Geometry and Computer Science, University of Innsbruck, email: manfred.husty@uibk.ac.at*
- *LARM, University of Cassino, Via Di Biasio 43, 03043 Cassino (Fr), Italy, email: ceccarelli@unicas.it*

Abstract: *This paper presents a workspace analysis of 3R industrial-type manipulators, which have geometrical simplification of general kinematic parameters. In particular, we have focused attention on industrial-type manipulators, which can be grouped usually as orthogonal and ortho-parallel manipulators. The classification regards with relative orientation of three directions of revolute joints' axes. A formulation is presented based on a level-set reconstruction of the workspace. The proposed analysis allows for determining different topologies of industrial manipulators based on kinematic properties. Numerical examples are shown.*

1. INTRODUCTION

Workspace analysis of serial manipulators is of great interest because of the influence of the workspace geometry on manipulator design, placement in a working environment, and trajectory planning.
Nowadays the majority of manipulators for industrial applications are of serial type. They often have geometric design simplifications, such as intersecting joint axes, orthogonal or parallel joint axes. Moreover, most of the industrial manipulators are wrist-partitioned, that is they consist of a concatenation of a 3R (Revolute) arm, i.e., regional structure, and a spherical wrist that is attached to the terminal link of the arm. The workspace analysis of such manipulators can be performed by considering the positioning and orienting task as well as the singularities separately.

Early studies have been developed for 3R manipulators for either positioning [1, 2]; or orienting tasks. An algebraic formulation for determining the workspace of 3R manipulators has been presented in [3] and then generalized for nR manipulators in [4].

The determination of the workspace boundary in Cartesian Space has been proposed also by [5].
Other papers are related to the singularity of the Jacobian matrix that is usually expressed in the Joint Space. Regions that are free of singularities in the Joint Space have been named C-sheets, [6]. In C-sheets it is possible to determine how to change posture without passing through singularities [7]. Manipulators that can change posture without meeting a singularity have been named cuspidal manipulators in [8]. The analysis and characterization of geometric singularities of the cross-section boundary curve was proposed in [9, 10].
Several authors have grouped manipulators into classes, as reported in [6, 8, 11], by considering special architectures, such as cuspidal or orthogonal manipulators, which have simplification in the architecture. In this paper we present a classification of 3R industrial-type manipulators as based on kinematic properties of the workspace, but not only on parameters simplifications. As a completely new method we discuss the level-set belonging to the two-parameter set of curves, which constitutes the cross-section of the workspace of the manipulator. The graph of the level-set directly linked to the level-set provides new and surprising insight in the internal structure of the workspace.

2. A FORMULATION FOR WORKSPACE ANALYSIS

A general 3R manipulator is sketched in Fig.1, in which the kinematic parameters are denoted by the Hartenberg and Denavit (H-D) notation. Without loss of generality the base frame is assumed to be coincident with $X_1Y_1Z_1$ frame when $\theta_1 = 0$, $a_0=0$ and $d_1=0$. The end-effector point H can be usually chosen as either the center of the end-effector, or the tip of a finger. Point H is placed on the X_3 axis at a distance a_3 from O_3, as shown in Fig.1. The general 3R manipulator is described by the H-D parameters a_1, a_2, d_2, d_3, α_1 and α_2, and θ_i, for (i = 1,…,3), as shown in Fig.1.
The position of point H with respect to reference frame $X_3Y_3Z_3$ can be represented by the vector $\mathbf{H}_3$. Using the transformation matrices T_i^{i+1}, the coordinates (x,y,z) of the operation point H with respect to the base frame $X_0Y_0Z_0$ are given by the position vector $\mathbf{H}_0$ in the form

$$\mathbf{H}_0 = T_0^1\, T_1^2\, T_2^3\, \mathbf{H}_3 \tag{1}$$

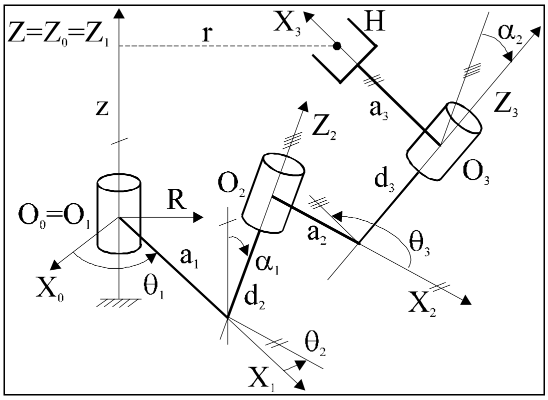

Fig. 1. A kinematic scheme for a general 3R manipulator.

The workspace of a general 3R manipulator can be expressed in the form of radial and axial reaches, r and z respectively, with respect to the base frame. r is the radial distance of point H from the Z_1-axis and z is the axial reach; both can be expressed as function of H-D parameters. Reaches r and z can be evaluated as function of coordinates if the position vectors in the form

$$r^2 = \left(H_0^x\right)^2 + \left(H_0^y\right)^2 = \left(H_1^x c\theta_1 - H_1^y s\theta_1\right)^2 + \left(H_1^x s\theta_1 + H_1^y c\theta_1\right)^2$$
$$z = H_0^z \tag{2}$$

which can be equivalently expressed in the form

$$r^2 = \left(H_1^x\right)^2 + \left(H_1^y\right)^2 \qquad z = H_1^z \tag{3}$$

Equation (3) represents a 2-parameter family of curves, which gives the cross-section workspace in a cross-section plane [1, 3] as function of the H-D parameters through H_1^x, H_1^y and H_1^z coefficients.

3. LEVEL-SET ANALYSIS FOR 3R MANIPULATORS

In the following this two-parameter set is interpreted as a level-set [12]. The level-set of a differentiable function $f : \Re^n \to \Re$ corresponding to a real value c is the set of points

$$\{(x_1,\dots x_n) \in \Re^n : (x_1,\dots x_n) = c\} \tag{4}$$

The potentiality of the level-set method is now applied to the workspace analysis of 3R manipulators. In particular, the level-set reconstruction for a serial manipulator can be obtained by using the 2 parameter-family of curves in Eq.(3).

The level-sets belonging to constant values of θ_3 are curves in the RZ-plane. Therefore, this one parameter set of curves can be viewed as the contour map of a surface S, which conveniently can be used to analyze the workspace of the manipulator. The surface S is defined via the functions

$$X^2 = r^2 \quad Y = z \quad Z = \tan\left(\frac{\theta_3}{2}\right) \tag{5}$$

By performing the half-tangent substitution v = tan (θ_2/2) in Eq.(5) and eliminating the v parameter one can obtain an implicit equation of the surface S.

$$S: F(X,Y,Z) = 0 \tag{6}$$

Equation (6) describes an algebraic surface which is of degree 20. It splits into two parts

$$F(X,Y,Z) = S_1(Z)\, S_2(X,Y,Z) \tag{7}$$

S_1 represents four double planes parallel to XY plane, in which the height depends on the H-D parameters.

S_2 is the graph of the level-set function. The parameter lines on this surface belong to θ_2 = const or θ_3 = const. Geometrically S is generated by taking a cross-section of the workspace that is parameterized by θ_2 and θ_3 and explode the overlapping level-set curves in the direction of the Z-axis.

The major advantage of this procedure is that on S one can see clearly the number of solutions of the Inverse Kinematics (IK) belonging to one point of the workspace cross-section.

In Fig.2 this is shown for a general design. In Fig.2a) the level-set curves are shown. It should be noted that in the displayed cross-section of the workspace in fact two different one-parameter sets of level-curves are displayed. The blue one belongs to θ_3 = const and the grey one belongs to θ_2 = const.

In the following we only discuss the blue set of curves. A discussion of the other set would lead to similar results.

On Fig.2b) and following 3D plots, a topologically equivalent surface to S is displayed, it is obtained by considering θ_3 on the Z-axis. Geometrically the level-set curves of Fig.2a) are the orthogonal projections of , the intersection curves with planes Z = const and the surface S onto the XY-plane. The blue level-set curves in Fig.2a) are therefore a contour map of the surface S. Additionally we have displayed in Fig.1b) a line parallel to the Z-axis. This line shows clearly four intersection points with the surface S. Therefore, the corresponding point in the level-set plane in Fig.2a) corresponds to a four fold solution of the IK. On the surface S_2 the θ_3 curves keep their closed curve nature and θ_2 ones are taken apart.

In order to determine the algebraic degree of S_2 one has to homogenize and intersect with the plane at infinity. The resulting intersection is completely independent of the H-D parameters. It consists of an eight fold line Z = 0 and two complex double lines. Thus, the surface is of algebraic degree 12.

Manipulators having singularities on the surface S can be considered as an algebraically closed set. Indeed, a small perturbation on H-D parameters will change the behavior of the manipulator. Singularities of the surface S can be found by considering the implicit equation of S, together with its partial derivatives with respect to X, Y, and Z, respectively [13]. All these four functions have to vanish for a point on the surface being singular. Singularity conditions can be expressed as functions of H-D dimensional parameters.

There is an important observation that can be made. Considering just the one parameter set of level-set curves in the plane of parameters r and z, one can observe singular points on the envelop curve of the set. These singular points have been discussed in the literature quite a lot.

An enumeration of all possible types of ring void has been presented in [9, 14] by analyzing the internal branch of the cross-section boundary envelope curve. The internal branch of the boundary envelope curve in the cross section R-Z shows generally 3 loops. The middle loop delimits a ring void and it is a part of the boundary curve; the others are related to 4-solution regions for the IK problem. By considering a formulation for the cross-section workspace boundary of 3R manipulators as proposed in [10] it is possible to determine the singularities on the inner boundary curve, which is a part of the enveloping curve. These singularities can be either double points or acnodes or cusps of the cross-section boundary curve [14].

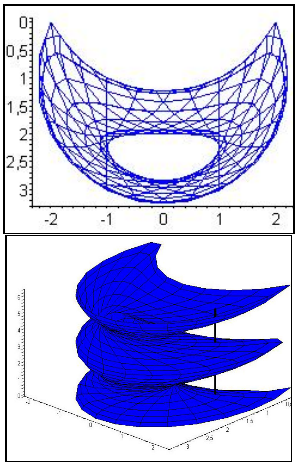

a) b)

Fig. 2. A numerical example for a general 3R manipulator: a) workspace cross-section; b) a topologically equivalent surface to S.

The graph S of the level-set function reveals a very different nature of these highly interesting singular points. Some of them arise just from the projection of S into the level-set plane and some of them come from singularities of the surface S. The geometrical interpretation for the singularities of the graph of the level-set function is that there is a value of θ_3 for which the operation point H lies on Z_2 axis. Therefore, there is a permanent singularity that causes a free motion about Z_2 axis, which is completely independent by θ_2 angle. In this paper we have focused our analysis on this kind of singularities for the 3R industrial type manipulators, which have been grouped in orthogonal and ortho-parallel manipulators.

A A Formulation for Orthogonal Manipulator

Orthogonal manipulators are characterized by having three revolute joint axes, which are orthogonal to each other. Therefore, kinematic parameters can be identified as a_1, a_2, a_3, d_2, d_3, twist angles $\square_1$ and $\square_2$ are set equal to -90 and 90 deg. Joint variables are identified as $\square_1$, $\square_2$ and $\square_3$, respectively, and they will be assumed unlimited in this work. A kinematic scheme is displayed in Fig. 3. The surface S of Eq.(6) has to be studied. In particular, the factors S_1 and S_2 of S can be analyzed separately.

For orthogonal manipulators the surface S_1 can be expressed in the form

$$S_1 = k_4 Z^4 + k_2 Z^2 + k_0 \quad , \tag{8}$$

where the coefficients k_i depend on a_2, a_3 and d_3 only. They can be expressed in the form

$$k_4 = (a_3 - a_2)^2 + d_3^2 ; \qquad k_0 = (a_3 + a_2)^2 + d_3^2$$
$$k_2 = 2(a_3 - a_2)(a_3 + a_2) + 2d_3^2 . \tag{9}$$

In general the equation for S_1 can have real solutions. The necessary and sufficient condition for having real solutions is: $d_3 = 0$ and $a_3 > a_2$. Other singularities can be found by analyzing surface S_2. Zeros of the set of equations $S_2 = 0$; $S_{2X} = 0$; $S_{2Y} = 0$; and $S_{2Z} = 0$, yield the geometric singularities of the surface S_2.

Singularities of S_2 surface can be can expressed by the product of two polynomials in the form

$$P_1 = d_3^2 + (a_3 - a_2)^2 ;$$
$$P_2 = \left(a_2^2 + a_3^2 + d_3^2\right)^2 - 4a_2^2 a_3^2 \tag{10}$$

The zeros of the set of equations: $S_2 = 0$; $S_{2X} = 0$; $S_{2Y} = 0$; and $S_{2Z} = 0$, yield the geometric singularities of S_2.

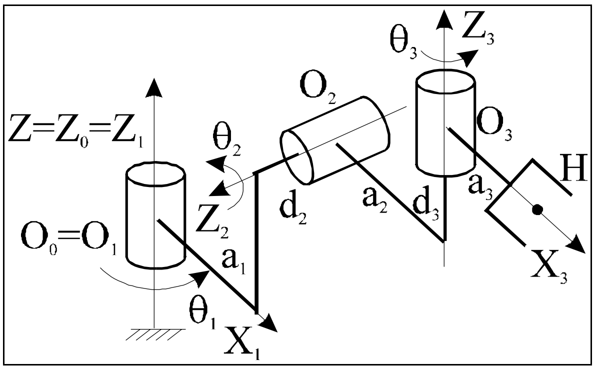

Fig. 3. A kinematic scheme for an orthogonal 3R manipulator.

A classification is considered in order to obtain groups of manipulators having similar kinematic properties. The following classes can be identified for orthogonal manipulators.

This classification allows obtaining design information related to workspace properties. Geometrically, when $\square_2$ is equal to 90 deg then a member of the $\square_3$ parameter set of curves belonging to different values of a_3 can intersect the Z_2 axis iff d_3 is equal to zero. In this case, the $\square_3$ parameter set of curves is in a plane containing Z_2 axis. In particular, each possible intersection of a $\square_3$ curve represents a singularity of the level-set graph. Only three cases can arise: no intersection, two distinct intersections and two coincident intersections. The three cases represent the three classes of industrial-type manipulators.

B A Formulation for Ortho-Parallel Manipulators

Ortho-parallel manipulators are characterized by having the first two revolute joint axes orthogonal to each other, and the last revolute joint axis is parallel to the second one. Therefore, kinematic parameters can be identified as a_1, a_2, a_3, d_2, d_3, and twist angles □$_1$ and □$_2$ are set equal to -90 and 0 deg. Joint variables are identified as □$_1$, □$_2$ and □$_3$, respectively, and they will be assumed unlimited in this work. A kinematic scheme is displayed in Fig. 4. The factors S_1 and S_2 of S are analyzed separately. S_1 can be expressed in the form

$$S_1 = k_2 Z^2 + k_0, \tag{11}$$

in which k_i coefficients depend on a_2 and a_3 only. They can be expressed in the form

$$k_2 = (a_3 - a_2)^2;\ k_0 = (a_3 + a_2)^2 \tag{12}$$

According to Decartes rule of signs a necessary and sufficient condition for having real solutions is iff there are changes in the signs of coefficients k_i. In particular, the number of real roots is equal to the number of changes of sign in the k_i coefficients. Therefore, S_1 has not real solutions. Other singularities can be found by analyzing surface S_2. Zeros of the set of equations $S_2 = 0$; $S_{2X} = 0$; $S_{2Y} = 0$; and $S_{2Z} = 0$, yield the geometric singularities of the surface S_2. Singularities of S_2 surface are given in the form

$$P_1 = (a_3 - a_2)^2 \tag{13}$$

Geometrically, when □$_2$ is equal to 0 deg then the □$_3$ parameter set of curves can intersect the Z_2 axis iff a_2 is equal to a_3. For this case, a □$_3$ curve is in a plane, which is orthogonal to Z_2 axis. Only two cases can arise: no intersection and two coincident intersections. These two cases yield two different classes of industrial-type manipulators. For the case under study the 2-parameter set of curves lies on a plane which is orthogonal to Z_2 and Z_3 axes.

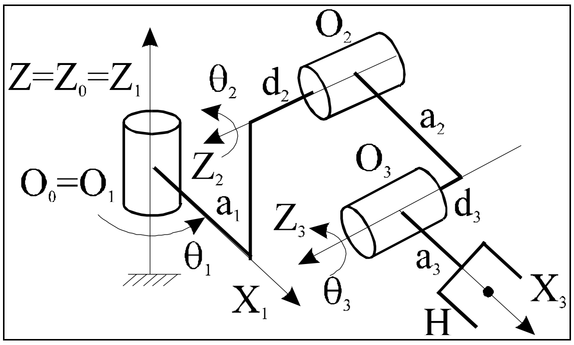

Fig. 4. A kinematic scheme for an ortho-parallel manipulator.

4. A CLASSIFICATION FOR 3R INDUSTRIAL-TYPE MANIPULATORS

According to the results that have been obtained for industrial-type manipulators, a classification can be proposed. The following groups contain all possible topologies of orthogonal and ortho-parallel manipulators, which can be characterized by the presence of singularities on the surface S. Furthermore, if the surface has real singularities then they also correspond to singularities of the cross-section of the boundary curve.

A. Class A: A General Industrial-Type Manipulator

A manipulator that belongs to the Class A has no (real) singularities on the surface S. It may have either a changing posture behavior or it can present a void within the workspace. A characteristic shape with corresponding cross-section Fig.s is reported in the examples of Figs. 5 and 6 for orthogonal manipulators, and Figs. 11 and 12 for ortho-parallel manipulators. Such general manipulators are characterized to have no singularities on the graph of the level-set. In addition, it can be observed that in general cuspidality behavior is not strictly related to special designs.

B. Class B Industrial-Type Manipulator

A manipulator that belongs to the Class B has only one singularity on the surface S. Class B manipulators can be characterized by the presence of 4-solution regions for the IK. The cross-section boundary curve for type B manipulators contains one acnode (hermit point) as singular point [14]. A Class B orthogonal manipulator is characterized by having $a_2 = a_3$; AND $d_3 = 0$. If $a_2 \le a_3$, the operation point H can meet the second joint axis whenever $\square_3 = \pm \arccos(-a_2/a_3)$, which was found also by [11].

Characteristic shapes with corresponding cross-sections for orthogonal manipulators are reported in the examples of Figs. 7 and 8. For class B orthogonal manipulators S_1 expression vanishes and singularities can be found by checking the singularities of S_2 polynomial expression. Type B orthogonal manipulators are characterized to have two coincident singular configurations that depend on $\square_3$ parameter only. A Class B ortho-parallel manipulator is characterized by having $a_2 = a_3$. Characteristic shapes with corresponding cross-sections for orthogonal manipulators are reported in the examples of Figs. 13 and 14.

C. Class C Industrial-Type Manipulator

This class of manipulators is characterized by having two distinct singularities on the surface S and in general 4-solution regions for the IK. Class C orthogonal manipulators have $a_3 > a_2$ AND $d_3=0$. The meaning of a singularity is that for a $\square_3$ value there exist a line passing through the operation point H and intersecting one of the manipulator axes. If d_3 is not equal to zero then the generating curve ($\square_3$) has not real solutions, OR if a_3 is less than a_2 than no singularities are on S surface. A characteristic shape and corresponding cross-sections are reported in the examples of Figs. 9 and 10.

Type C manipulators can have a void iff the projections of the singularities of the S surface belong to the workspace boundary too. In the two singularities point H meets the second joint axis and the manipulator has infinite IK solutions [10]. It has been found that ortho-parallel manipulators cannot have two distinct singularities. It can be verified both from the geometrical interpretation and formulation.

5. NUMERICAL EXAMPLES

In this Section numerical examples are presented for orthogonal and ortho-parallel manipulators in Figs. 5 to 14. In particular, Fig.s 5 and 6 show two examples for Class A manipulators, for which the surface S has not singularities. The corresponding cross-section boundary curve can have only cusps and/or double points, as it is shown in the two examples. In particular, in Fig. 5c) a Cartesian representation of the two-parameter family of curves is shown and a $\square_3$-curve is shown in red.

Fig. 7 shows a numerical example for Class B manipulators. The manipulator has only one singularity of the S surface. It is worth noting that the singularity arises for a value of the $\square_3$ angle and geometrically it corresponds to the configuration in which the operation point H lies on the Z_2 axis. The geometrical interpretation of the singular configuration is that a $\square_3$-curve is tangent to the Z_2 axis, as shown in Fig. 7c).

Fig. 8 shows a numerical example for a Class B orthogonal manipulator. The manipulator has only one singularity for the S surface, as shown in Fig. 8b). The inner part of the cross-section boundary curve is characterized by the presence of one acnode and two cusps as singularities of the curve.

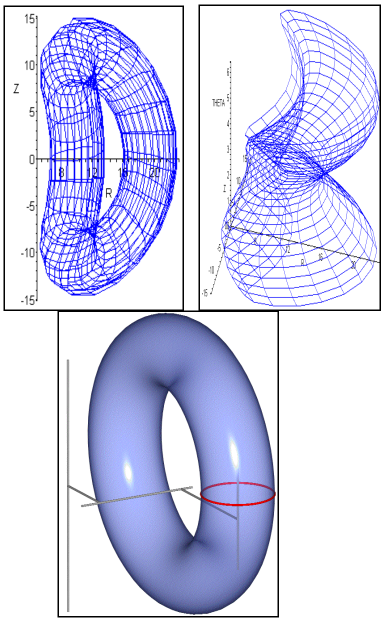

a) b) c)

Fig. 5. A numerical example of Class A orthogonal manipulators with void, a_1=6.17, a_2=10.90, a_3=3.49, d_2=8.80, d_3=2.52; a) workspace cross-section; b) topologically equivalent surface to S; c) a representation in Cartesian space of the two-parameter family of curves in Eq.(3) (a $\square_3$-curve is represented in red).

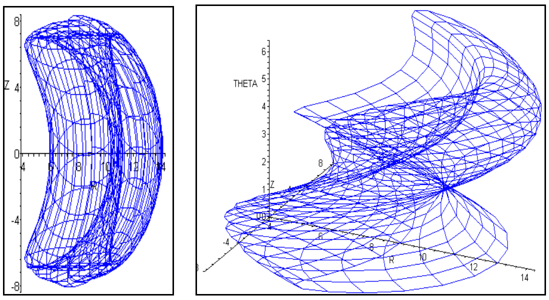

a) b)

Fig. 6. A numerical example of Class A orthogonal manipulators without void, a_1=2.61, a_2=0.97, a_3=3.12, d_2=7.21, d_3=6.92; a) workspace cross-section; b) topologically equivalent surface. (u is unit length and angles are in radians)

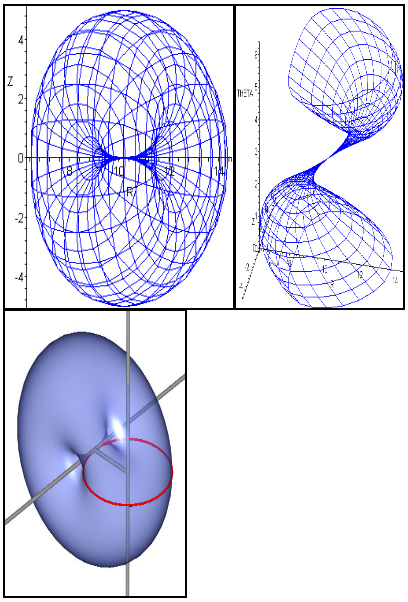

a) b) c)

Fig. 7. A numerical example of Class B orthogonal manipulators, a_1=6.00, a_2=a_3=2.51, d_2=8.22; a) workspace cross-section; b) topologically equivalent surface to S; c) a representation in Cartesian space of the two-parameter family of curves in Eq.(3) (a $\square_3$ -curve is represented in red).

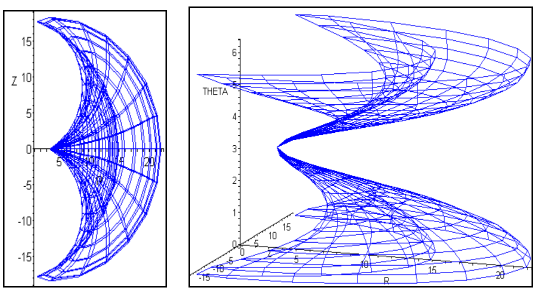

a) b)

Fig. 8. A numerical example of Class B orthogonal manipulators, a_1=3.52, a_2=a_3=9.19, d_2=0.393; workspace cross-section; b) topologically equivalent surface to S.

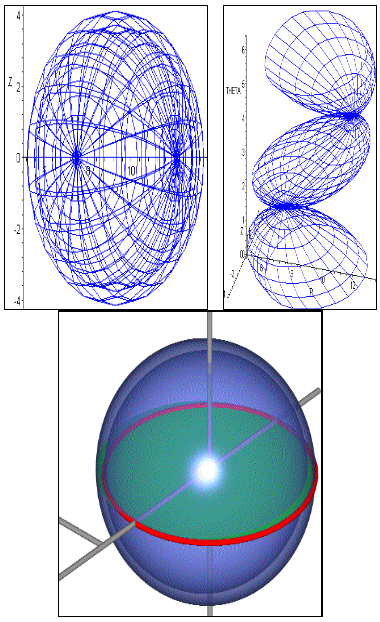

a) b)

Fig. 9. A numerical example of Class C orthogonal manipulators with void, a_1=7.29, a_2=0.203, a_3=3.943, d_2=5.70: a) workspace cross-section; b) topologically equivalent surface to S; c) a representation in Cartesian space of the two-parameter family of curves in Eq.(3) (a $\square_3$-curve is represented in red).

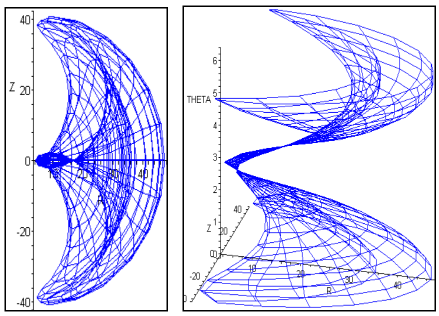

a) b)

Fig. 10. A numerical example of Class C orthogonal manipulators, a_1=5.77, a_2=19.20, a_3=21.45, d_2=6.31: a) workspace cross-section; b) topologically equivalent surface to S. (u is unit length and angles are in radians)

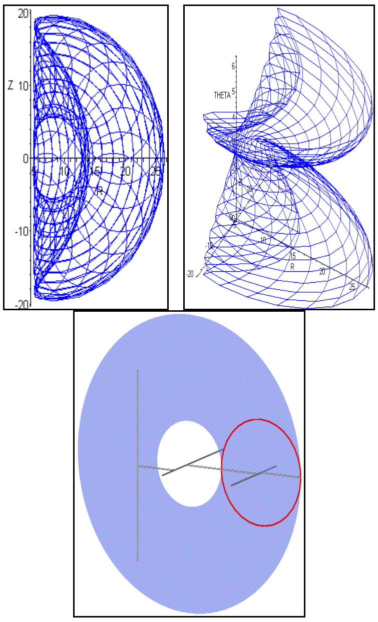

a) b) c)

Fig. 11. A numerical example for Class A ortho-parallel manipulators without void, a_1=6.39, a_2=12.60, a_3=6.98, d_2=4.04, d_3=0.957; a) workspace cross-section; b) topologically equivalent surface; c) a representation in Cartesian space of the two-parameter family of curves in Eq.(3)

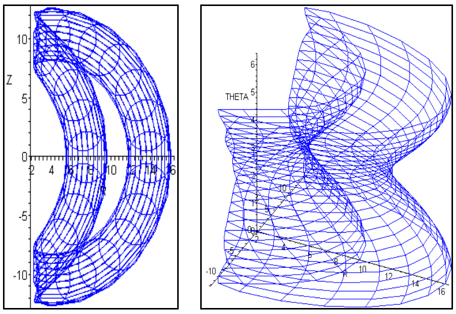

a) b)

Fig. 12. A numerical example for Class A ortho-parallel manipulators with void, a_1=3.28, a_2=10.50, a_3=2.20, d_2=1.69, d_3=0.492; a) workspace cross-section; b) topologically equivalent surface to S.

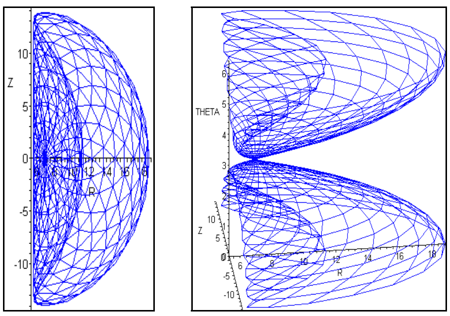

a) b)

Fig. 13. A numerical example for Class B ortho-parallel manipulators, a_1=4.04, a_2=a_3=6.98, d_2=0.957, d_3=4.64; a) workspace cross-section; b) topologically equivalent surface to S.

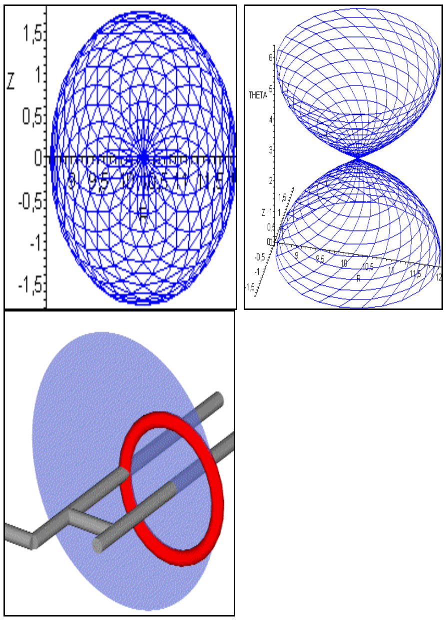

a) b)

Fig. 14. A numerical example for Class B ortho-parallel manipulators, a_1=9.99, a_2=a_3=0.875, d_2=0.938, d_3=1.54; a) workspace cross-section; b) topologically equivalent surface to S; c) a representation in Cartesian space of the two-parameter family of curves in Eq.(3) (a $\square_3$ curve is represented in red).

Fig. 9 shows a numerical example for Class C manipulators. It is worth noting that there are two distinct singularities for the graph of the level set, as shown in Fig. 9b) and the cross-section boundary curve has 2 acnodes. The manipulator has 2 and 4 solution regions for the IKP. Acnodes that appear in the cross-section boundary curve can be identified as singularities of the S surface. The geometrical interpretation is shown in Fig. 9c) in which it is possible to note that a $\square_3$ -curve (in red) intersects the Z_2 axis into two distinct points.

Fig. 10 shows a numerical example for the Class C manipulators in which one of the singularities of the S surface is a double point for the cross-section boundary curve.

Fig.s 11 and 12 show numerical examples for Class A ortho-parallel manipulators, with and without void.

Fig.s 13 and 14 show numerical examples for Class B ortho-parallel manipulators, which have only one singularity on the S surface. In Fig.14c) the $\square_3$-curve (in red) is tangent to the Z_2 axis. This configuration gives the singularity of the S surface, as shown in Fig. 14b), and acnode in the workspace cross section boundary curve.

6. CONCLUSION

This paper presents a novel analysis of the workspace for industrial-type manipulators based on the level-set reconstruction of the workspace. The method allows to determine useful information for characterization of the workspace in Cartesian Space. Singularities on the graph S of the level-set are singular configurations in which there is a value of $\square_3$ angle for which the manipulator encounters a permanent singularity. Geometrical interpretations for the singularites are given. Futhermore, the proposed formulation allows to avoid design conditions having this type of singularities.

REFERENCES

[1] Freudenstein F., Primrose E.J.F., On the Analysis and Synthesis of the Workspace of a Three-Link, Turning-Pair Connected Robot Arm, *ASME Jnl of Mech., Transm. and Autom. in Design*, vol.106, pp. 365-370, 1984.

[2] Roth B., Performance Evaluation of Manipulators From a Kinematic Viewpoint, *National Bureau of Standards Special Publication*, No. 459, pp. 39-61, 1975.

[3] Ceccarelli M., On the Workspace of 3R Robot Arms, *Proc. 5th IFToMM Int. Symp. on Theory and Practice of Mechanism*, Bucharest, Vol. II-1, pp. 37-46, 1989.

[4] Ceccarelli M., A Formulation for the Workspace Boundary of General N-Revolute Manipulators, *Mech. and Machine Theory*, vol.31, no.5, pp. 637-646, 1996.

[5] Smith D.R., Lipkin H., Higher Order Singularities of Regional Manipulators, *Proc. IEEE Int. Conf. on Rob. and Autom.*, vol.1, pp. 194-199, 1993.

[6] Burdick, J.W., A Classification of 3R Regional Manipulator Singularities and Geometries, *Mech. and Machine Theory*, vol.30, no.1, pp. 71-89, 1995.

[7] Parenti-Castelli V., Innocenti C., Position Analysis of Robot Manipulators: Regions and Sub-Regions, *on Advances in Robot Kinematics*, Ljubljana, pp.150-158, 1988.

[8] Wenger P., Some Guidelines for the Kinematic Design of New Manipulators, *Mech. and Machine Theory*, vol.35, no.3, pp.437-449, 2000.

[9] Ottaviano E., Ceccarelli M., Lanni C., A Characterization of Ring Void in Workspace of Three-Revolute Manipulators, *Proc. 10th World Congress on the Theory of Machines and Mechanisms*, Oulu, vol.3, pp. 1039-1044, 1999.

[10] Ottaviano E., Husty M., Ceccarelli M., A Cartesian Representation for the Boundary Workspace of 3R Manipulators, in*: Advances in Robot Kinematics*, Sestri Levante, pp. 247-254, 2004.

[11] Zein M., Wenger P., Chablat D., An Exhaustive Study of the Workspaces Topologies of All 3R Orthogonal Manipulators with Geometrical Simplifications, *Proc. Of CK2005, 12th International Workshop on Computational Kinematics*, paper 34-CK2005, 2005.

[12] Sethian J.A., Level-Set Methods and Fast Marching Methods, Cambridge University Press, 1996.

[13] Gibson C.G., Elementary Geometry of Algebraic Curves, Cambridge University Press, 1998.

[14] Ottaviano E., Husty M., Ceccarelli M., Identification of the Workspace Boundary of a General 3-R Manipulator, *ASME Journal of Mechanical Design*, Vol. 128, N.1, pp. 236-242, 2006.